Sustainable heterologous production of terpene hydrocarbons in cyanobacteria

Cinzia Formighieri & Anastasios Melis

Photosynthesis Research
Official Journal of the International Society of Photosynthesis Research

ISSN 0166-8595
Volume 130
Combined 1-3

Photosynth Res (2016) 130:123-135
DOI 10.1007/s11120-016-0233-2

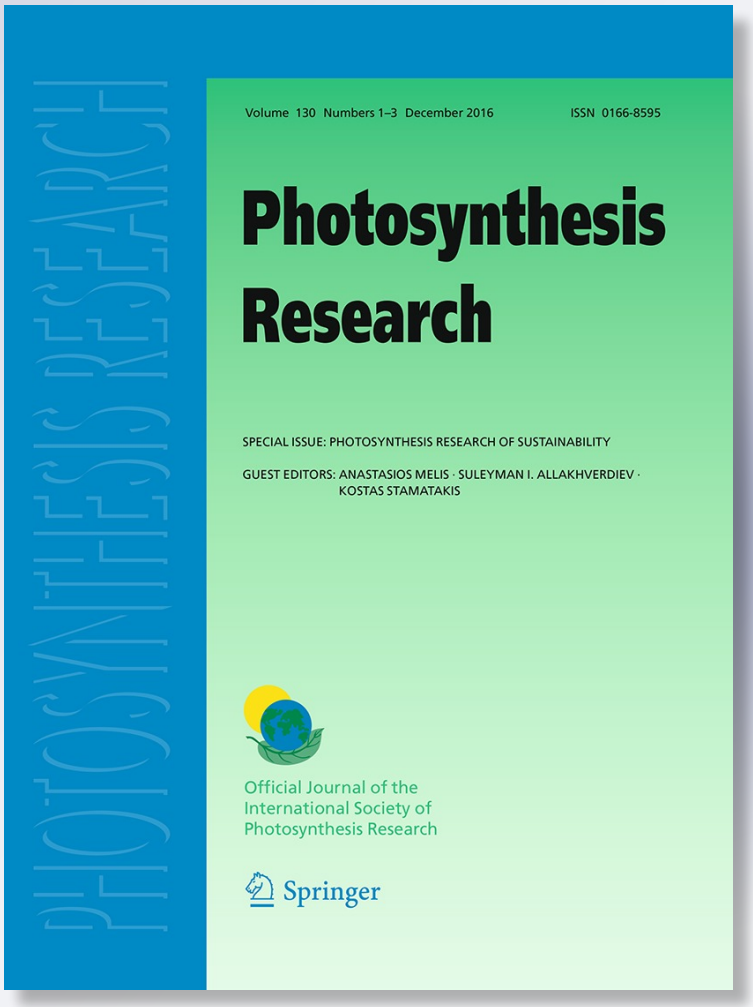

Springer

Photosynth Res (2016) 130:123–135
DOI 10.1007/s11120-016-0233-2

ORIGINAL ARTICLE

Sustainable heterologous production of terpene hydrocarbons in cyanobacteria

Cinzia Formighieri[1] · **Anastasios Melis**[1]

Received: 7 December 2015 / Accepted: 11 February 2016 / Published online: 19 February 2016

Abstract Cyanobacteria can be exploited as photosynthetic platforms for heterologous generation of terpene hydrocarbons with industrial application. However, the slow catalytic activity of terpene synthases ($k_{cat} = 4\ s^{-1}$ or slower) makes them noncompetitive for the pool of available substrate, thereby limiting the rate and yield of product generation. Work in this paper applied transformation technologies in *Synechocystis* for the heterologous production of β-phellandrene (monoterpene) hydrocarbons. Conditions were defined whereby expression of the β-phellandrene synthase (PHLS), as a CpcB·PHLS fusion protein with the β-subunit of phycocyanin, accounted for up to 20 % of total cellular protein. Moreover, CpcB·PHLS was heterologously co-expressed with enzymes of the mevalonic acid (MVA) pathway and geranyl-diphosphate synthase, increasing carbon flux toward the terpenoid biosynthetic pathway and enhancing substrate availability. These improvements enabled yields of 10 mg of β-phellandrene per g of dry cell weight generated in the course of a 48-h incubation period, or the equivalent of 1 % β-phellandrene:biomass (w:w) carbon-partitioning ratio. The work helped to identify prerequisites for the efficient heterologous production of terpene hydrocarbons in cyanobacteria: (i) requirement for overexpression of the heterologous terpene synthase, so as to compensate for the slow catalytic turnover of the enzyme, and (ii) enhanced endogenous carbon partitioning toward the terpenoid biosynthetic pathway, e.g., upon heterologous co-expression of the MVA pathway, thereby supplementing the native metabolic flux toward the universal isopentenyl-diphosphate and dimethylallyl-diphosphate terpenoid precursors. The two prerequisites are shown to be critical determinants of yield in the photosynthetic CO_2 to terpene hydrocarbons conversion process.

Keywords Metabolic engineering · Monoterpene hydrocarbons · Mevalonic acid pathway · β-Phellandrene · Phycocyanin · *Synechocystis*

Abbreviations

dcw	Dry cell weight
DMAPP	Dimethylallyl-diphosphate
GPP	Geranyl-diphosphate
GPPS	Geranyl-diphosphate synthase
IPP	Isopentenyl-diphosphate
MEP	2-C-Methyl-D-erythritol 4-phosphate
MVA	Mevalonic acid
PHL	β-Phellandrene
PHLS	β-Phellandrene synthase

Introduction

Plant essential oils, such as monoterpene hydrocarbons, are naturally synthesized and accumulate in specialized plant structures, the trichomes, by a number of terrestrial plant species. These compounds have commercial value as synthetic chemistry feedstock, in the pharmaceutical and

Electronic supplementary material The online version of this article (doi:10.1007/s11120-016-0233-2) contains supplementary material, which is available to authorized users.

✉ Anastasios Melis
melis@berkeley.edu

[1] Department of Plant and Microbial Biology, University of California, 111 Koshland Hall, Berkeley, CA 94720-3102, USA

cosmetic industries, in personal-care products, household and industrial cleaning supplies, and as advanced biofuels (Demissie et al. 2011; Harvey et al. 2010; Tracy et al. 2009). Traditionally, essential oils are obtained from the plant biomass, but fluctuations in feedstock supply, high cost of extraction, and the increasing product demand have prompted the development of heterologous microbial systems for monoterpene hydrocarbons production (Duetz et al. 2003). These include heterotrophic bacteria and yeast (Alonso-Gutierrez et al. 2013; Fischer et al. 2011; Formighieri and Melis 2014a; Sarria et al. 2014), and photosynthetic cyanobacteria (Davies et al. 2014; Formighieri and Melis 2015). Monoterpene hydrocarbons were found to spontaneously separate from the cyanobacterial biomass and the extracellular aqueous medium, and to accumulate as floater molecules on the surface of sealed cultures, where they were easily siphoned off (Bentley et al. 2013; Davies et al. 2014; Formighieri and Melis 2015). The spontaneous product separation from the biomass and the liquid culture positively impacts the economics of the microbial production process, facilitating product segregation and harvesting, and alleviating potential inhibitory or toxic effects of the product on cellular metabolism and fitness. In contrast to heterotrophic microorganisms that require supply of exogenous organic carbon for growth, cyanobacteria are attractive for their ability to directly convert sunlight into chemical energy through the process of photosynthesis, and for the possibility of diverting photosynthesis-associated carbon metabolism toward the biosynthesis of desired chemicals. Growth of cyanobacteria on a large scale would not exert pressure on the availability of agricultural land and on the price/availability of sugar feedstocks (Stephens et al. 2013).

Typically, cyanobacteria and other aquatic organisms do not have the ability to generate monoterpene hydrocarbons, or other plant essential oils, as they lack the terpene synthase genes required for their synthesis (Van Wagoner et al. 2007). On the other hand, previous work from this lab has shown that heterologous expression of the *Lavandula angustifolia* (lavender) β-phellandrene (monoterpene) synthase (PHLS) in the cyanobacterium *Synechocystis* endowed the cells with constitutive photoautotrophic generation of β-phellandrene, offering the proof-of-concept that cyanobacteria can be exploited as photosynthetic platforms for heterologous production of terpene hydrocarbons for industrial application (Bentley et al. 2013; Formighieri and Melis 2014b, 2015). However, terpene synthases were shown to have a slow k_{cat} (4 s^{-1}, or slower) (Demissie et al. 2011; Schilmiller et al. 2009; Rajaonarivony et al. 1992). This is consistent with the much slower (about 1/30th) catalytic activity of secondary metabolism enzymes, compared to those of the primary metabolism (Bar-Even et al. 2011). While preference for a slow k_{cat} may be desirable in the context of physiological regulation of essential oil synthesis in plants, this parameter becomes counterproductive in the heterologous production of terpene hydrocarbons for industrial application. A slow k_{cat} can be overcome using a correspondingly higher concentration of the terpene synthase enzyme (e.g., PHLS), as the prerequisite, which can help to alleviate rate and yield limitations and to generate meaningful quantities of product (Formighieri and Melis 2015).

In more detail, the substrate for β-phellandrene synthesis is geranyl-diphosphate (GPP), and the reaction is catalyzed by the enzyme β-phellandrene synthase (PHLS). In turn, GPP is synthesized upon the covalent linkage of isopentenyl-diphosphate (IPP) to dimethylallyl-diphosphate (DMAPP), which serve as the universal reactants to all terpenoids synthesized by the living cell, including carotenoids, phytol, quinone prenyl tails, and so on. Heterologously expressed PHLS needs to efficiently compete with the endogenous terpenoids pathway for the limited supply of carbon substrate, and high levels of PHLS enzyme concentration are required to compensate for its slow k_{cat}.

Use of strong promoters was shown to be necessary but not sufficient to achieve high levels of PHLS expression (Formighieri and Melis 2014b). In particular, expression of PHLS under the strong endogenous *cpc* operon promoter resulted in protein levels that were low (less than 1 % of the total cellular protein), and nowhere near those of the native phycocyanin subunits, which are expressed under the same promoter (Formighieri and Melis 2014b). The limitation in the amount of PHLS was later overcome upon overexpression of the PHLS protein as a fusion protein to the highly abundant in cyanobacteria phycocyanin β-subunit (CpcB), which was necessary and sufficient to express the recombinant protein up to 20 % of total cell protein and, thereby, to alleviate limitations in the rate of β-phellandrene production due to low enzyme concentration (Formighieri and Melis 2015).

An additional limitation in β-phellandrene synthesis is encountered in the highly regulated carbon flux through the endogenous terpenoid biosynthetic pathway, which accounts for only 4–5 % of all photosynthetically fixed carbon in cyanobacteria (Lindberg et al. 2010; Melis 2013). Cyanobacteria naturally express the methyl-erythritol-4-phosphate (MEP) pathway (Lichtenthaler 2000) that supplies the endogenous terpenoids biosynthesis with the IPP and DMAPP universal precursors. Efforts to enhance carbon flux through the MEP pathway in bacteria were met with limited success (Farmer and Liao 2001; Kim and Keasling 2001; Matthews and Wurtzel 2000). In contrast to the MEP pathway, which is of prokaryotic origin and active in most bacteria, algal, and plant plastids, the mevalonic acid (MVA) pathway naturally operates in the cytosol of eukaryotes, Archae, and some bacteria, and it also

generates DMAPP and IPP for terpenoid synthesis. Heterologous expression of the MVA pathway in fermentative bacteria was shown to be a good strategy by which to enhance carbon flux through the terpenoid biosynthetic pathway and thus to increase the pool size of IPP and DMAPP in the cell (Martin et al. 2003; Zurbriggen et al. 2012; Alonso-Gutierrez et al. 2013; Formighieri and Melis 2014a). In cyanobacteria, two polycistronic MVA pathway constructs with genes derived from *Enterococcus faecalis* and *Streptococcus pneumoniae* were heterologously expressed in *Synechocystis* (Bentley et al. 2014), helping to enhance rates of isoprene production and showing for the first-time applicability and function of the MVA pathway in a photosynthetic microorganism. However, in this important concept validation (Bentley et al. 2014), the terpene synthase enzyme was expressed at low levels, a condition that limited the rate and yield of product formation.

In the present study, we investigated the molecular and mechanistic aspects responsible for the accumulation (20 % of total cell protein) of the CpcB·PHLS fusion, compared to PHLS in a nonfusion configuration. Included in this investigation are assessments on transgene transcription, protein synthesis, and protein stability. Moreover, we addressed the limitation imposed by the low IPP/DMAPP pool size on the rate and yield of β-phellandrene synthesis. This was achieved by co-expressing in *Synechocystis* the codon-optimized heterologous enzymes of the MVA pathway and a geranyl-diphosphate synthase (GPPS) along with the construct overexpressing the CpcB·PHLS fusion protein. Positive results of the enhanced rate and yield of β-phellandrene synthesis informed about the validity of enzyme concentration and endogenous substrate flux in the heterologous synthesis of monoterpene hydrocarbons.

Materials and methods

Synechocystis strains, recombinant constructs, and culturing conditions

Synechocystis sp. PCC 6803 (*Synechocystis*) was used as the experimental strain and referred to as the wild type (wt) in this study. Expression of the codon-optimized β-phellandrene synthase from *L. angustifolia* (lavender) was employed for β-phellandrene generation by *Synechocystis* transformants, as described (Formighieri and Melis 2015). *Synechocystis* codon-optimized genes for the upper and lower MVA pathway were derived from *E. faecalis* and *S. pneumoniae* (Zurbriggen et al. 2012) and cloned as two separate operons (Bentley et al. 2014). Genes for the upper MVA pathway were flanked by 500 bp of upstream and downstream *psbA2* sequences for homologous recombination in the *Synechocystis* genome, plus a kanamycin resistance gene as selectable marker. Genes for the lower MVA pathway were flanked by 500 bp of upstream and downstream *glgA1* sequences for homologous recombination, plus a spectinomycin resistance gene as selectable marker. The heterologous Ptrc promoter (Formighieri and Melis 2014b) was employed for driving transgene expression, and the codon-optimized *GPPS2* gene from *Picea abies* (Formighieri and Melis 2014a) was additionally cloned upstream of the lower MVA genes in the *glgA1* operon. Gene sequences of constructs used in this study are reported in the Supplementary material.

Synechocystis transformations were made according to established protocol (Williams 1988; Eaton-Rye 2011). Wild type and transformants were maintained on 1 % agar BG11 media supplemented with 10 mM TES-NaOH (pH 8.2) and 0.3 % sodium thiosulfate. Liquid cultures in BG11 were buffered with 25 mM phosphate (pH 7.5) and incubated under continuous low-stream bubbling with air at 28 °C. Transgenic DNA copy homoplasmy was achieved with cells incubated on agar in the presence of the antibiotic selection.

Genomic DNA PCR analysis of *Synechocystis* transformants

Genomic DNA templates were prepared with Chelex®100 Resin (BioRad), as described (Formighieri and Melis 2014b). The following oligonucleotide primers were used to map transgene insertion in the *Synechocystis* genome, and to test for DNA copy homoplasmy: cpc_us, cpcA_Rv, PHLS_Rv, psbA2_us, psbA2_ds, HMGS_Rv, glgA1_us, glgA1_ds, FNI_Rv. The location of these primers on the genomic DNA is shown in Figs. 1 and 4. The respective oligonucleotide sequences are given in the Supplementary material, Table 1S.

Transcript analysis

Total RNA was prepared from *Synechocystis* cells using the TRIzol®Reagent (Invitrogen), according to the manufacturer's instructions. After DNA digestion with DNaseI (Fermentas), the RNA was reverse-transcribed from random hexamers (Invitrogen) by the SuperScript® III Reverse Transcriptase (Invitrogen). For the RT-qPCR, 10 ng of cDNA were used as template. Primers were designed within the PHLS encoding region to amplify a 113 bp DNA fragment at the 3′ end (PHLS1_Fw and PHLS1_Rv primers) or a 137 bp DNA fragment toward the 5′ end (PHLS2_Fw and PHLS2_Rv primers). DNA amplification was monitored by SYBR Green fluorescence (SsoAdvanced™ Universal SYBR® Green Supermix, Bio-Rad). Analysis of relative gene expression data was performed using the $\Delta\Delta C_T$ method (Livak and Schmittgen 2001). The relative abundance of *rnpB* was used as internal control

(rnpB_Fw and rnpB_Rv primers). All oligonucleotide primer sequences are reported in the Supplementary material, Table 1S.

For the polyribosome analysis, exponentially growing cultures were incubated for 15 min with 5 μg/mL kanamycin in order to stop mRNA translation. Cultures were then cooled to 4 °C and centrifuged at 6000×*g* for 10 min. The cell pellet was resuspended in chilled buffer (50 mM Tris-HCl pH 8.2, 50 mM KCl, 25 mM $MgCl_2$, 10 mM EGTA, 5 mM DTT, and 5 μg/mL kanamycin), frozen then thawed in ice water, and disrupted by passing through a French Press at 20,000 psi. Nonidet P40 was added to the lysates at a final concentration of 0.5 % v/v. Following centrifugation at 20,000×*g* for 10 min, the cleared lysate supernatant was loaded on a 10–40 % w/v continuous sucrose gradient and centrifuged at 122,000×*g* for 5 h in a Beckman SW27 rotor at 4 °C. Gradients were fractionated in 10 equal fractions. After removal of the first and the last fractions, total RNA was extracted from the remaining fractions and analyzed by semi-quantitative RT-PCR. The signal intensity of the RT-PCR product, when the PCR reaction was terminated before saturation, was found to depend on the abundance of the target transcript in the sucrose gradient fraction. In particular, 8 μL for each RNA sample were reverse transcribed in 20 μL reactions, and 3 μL were used as templates for the PCR reaction. *cpcB* and *PHLS* were amplified with either cpcB_Fw and cpc_Rv primers or PHLS_Fw and PHLS_Rv primers, respectively (Supplementary material, Table 1S).

Protein analysis

Protein extraction from cell lysates was performed as described (Formighieri and Melis 2015). For the time-course analysis of protein stability upon protein synthesis inhibition, cultures at $OD_{730\ nm}$ of ~0.9 were treated with 50 μg/mL of kanamycin to inhibit protein synthesis. Cellular proteins were extracted prior to the kanamycin treatment, and after incubation for 5, 24, and 96 h. For Western blot analysis, SDS-PAGE resolved proteins were transferred from the polyacrylamide gel to a nitrocellulose membrane and probed with either PHLS (Bentley et al. 2013) or D1 (Kirst et al. 2014) antibodies. Specific antibodies recognizing individual enzymes of the MVA pathway and the GPPS2 were raised in rabbit, as previously described (Zurbriggen et al. 2012; Formighieri and Melis 2014a).

Quantification of β-phellandrene production by *Synechocystis* transformants

β-Phellandrene production and separation from *Synechocystis* cultures were performed as described (Bentley et al. 2013; Formighieri and Melis 2014b, 2015). Typically, cells from mid-growth cultures were pelleted and resuspended in fresh medium at $OD_{730\ nm} = 0.5$, bubbled with 100 % CO_2 to fill the gaseous headspace of the gaseous–aqueous two-phase reactor (Bentley and Melis 2012), sealed, and incubated for 48 h in the light. Since β-phellandrene spontaneously diffuses out of the cells, and cells were pelleted and resuspended in fresh media, β-phellandrene concentration at the beginning of the incubation period was zero. At the end of the 48-h incubation, β-phellandrene was collected as a floater molecule, siphoned off from the surface of the cultures upon the application of a known amount of hexane over-layer, and measured by absorbance spectrophotometry and sensitive gas chromatography (GC-FID) (Formighieri and Melis 2014a; 2014b). The amount of β-phellandrene generated by the culture was normalized to the dried biomass (w:w) that was produced during the same 48-h incubation period in the light (g of dry cell weight after 48-h growth minus g of dry cell weight of the starting biomass upon culture inoculation). This approach is slightly different from the practice in our previous publications (Formighieri and Melis 2014b, 2015), where β-phellandrene yields were expressed as mg of product normalized to the total biomass collected at the end of the 48-h incubation period.

Accession numbers

Accession numbers of genes used in this study are as follows: HMGS (AAO81154.1), HMGR (AAO81155.1), ATOB (AKK18188.1), MK (AAK99142.1), PMD (AAK 99143.1), PMK (AAK99144.1), FNI (AAK99145.1), GPPS2 (EU432047.2), LaPHLS (HQ404305), CpcB (AGF50 922.1).

Results

Amplification of PHLS expression in cyanobacteria

The *cpc* operon promoter controls expression of the abundant phycocyanin subunits and their associated linker polypeptides of the phycobilisome light-harvesting antenna (Fig. 1a). This endogenous strong promoter was employed to drive heterologous expression of the codon-optimized *PHLS* gene upon deletion and replacement of all the *cpc* operon genes (Fig. 1b). In addition, the *PHLS* gene was expressed under the same promoter as a fusion with *cpcB*, while keeping the downstream *cpc* operon genes in place (Fig. 1c).

Real Time RT-qPCR analysis was employed to compare transcript levels of the *PHLS* transgene, when expressed by itself (Fig. 1d, PHLS), to those of the *cpcB·PHLS* fusion

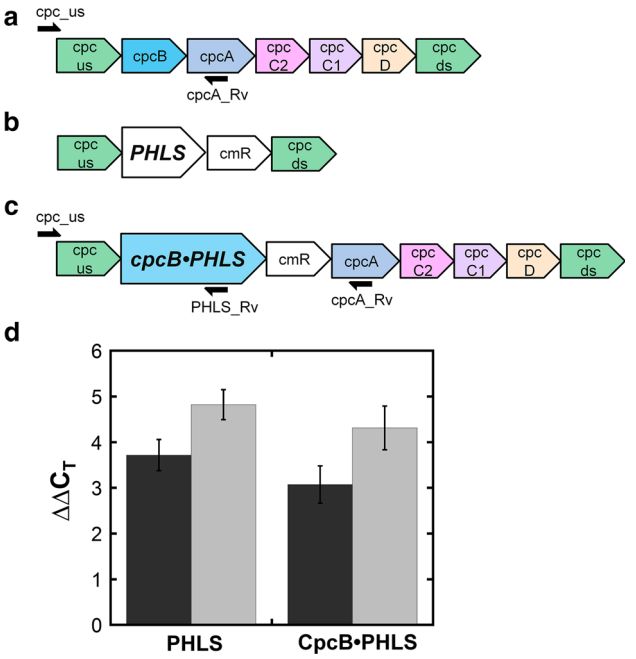

Fig. 1 Schematic of the wt *cpc* operon locus and of the *PHLS* recombinant constructs expressed in *Synechocystis* transformants. **a** The *cpc* operon locus encoding the abundant β-subunit (cpcB) and α-subunit (cpcA) of phycocyanin along with the phycocyanin peripheral rod linker polypeptides (cpcC2, cpcC1, and cpcD). **b** The *PHLS* gene along with the chloramphenicol resistance cassette (cmR), expressed under the control of the endogenous *cpc* promoter upon replacement of the *cpc* operon. **c** The *PHLS* transgene fused to the endogenous *cpcB* gene of *Synechocystis,* with the fusion construct expressed under the control of the *cpc* promoter. Note that the rest of the *cpc* operon genes (*cpcA* through *cpcD*) are on the 3′ end of the chloramphenicol resistance cassette (cmR). *Arrows* in **a** and **c** mark the position of oligonucleotide primers used in the PCR analysis of the transformants. **d** Transcript steady-state levels of *PHLS* and *cpcB·PHLS* were measured by real time RT-qPCR and normalized to the expression of the *rnpB* gene as internal control. Two different sets of primers were employed, one from the 3′end of the *PHLS* encoding sequence (*black bars*) and the other from the 5′ end of the *PHLS* encoding sequence (*gray bars*). Results from three independent transformant lines were averaged in the analysis of each genotype

construct (Fig. 1d, CpcB·PHLS). In this quantitative analysis, primers for the Real Time RT-qPCR reactions were selected from the 3′end or the 5′end of the *PHLS* transgene (Fig. 1d, black and gray bars, respectively). As shown in Fig. 1d, the *PHLS* and *cpcB·PHLS* transgene constructs resulted in about equal rates of transcription and showed comparable steady-state levels of *PHLS* versus *cpcB·PHLS* mRNA. It is concluded that the *cpc* operon promoter is equally effective in driving transcription of the *PHLS* and *cpcB·PHLS* gene constructs.

Protein synthesis was later investigated by analyzing the polyribosomes distribution profile associated with the *PHLS* and *cpcB·PHLS* transcripts. This experiment was performed upon polyribosome isolation following a sucrose gradient ultracentrifugation, seeking to test for differences in the rate of translation of the corresponding mRNAs (Fig. 2). This analysis is based on the fact that, in actively growing cells, multiple ribosomes simultaneously engage in the translation of the same mRNA. The rate and efficiency of translation is determined by the rate and efficiency of ribosome migration on the mRNA molecule (Qin and Fredrick 2013). A high density of polyribosomes in prokaryotes is attributed to a ribosome piling-up, when a slower ribosome migration rate on the mRNA causes multiple ribosomes to associate with the same mRNA molecule (Qin and Fredrick 2013). Conversely, a low density of polyribosomes is attributed to efficient ribosome migration on the mRNA, resulting in efficient translation and high protein accumulation (Qin and Fredrick 2013).

Polyribosomes can be resolved by sucrose-density gradient ultracentrifugation, since each ribosome adds substantial mass to the complex (Qin and Fredrick 2013). The results of Fig. 2 are representative of three independent biological replicates and showed that transcripts from the *PHLS* construct were associated about evenly with low-density and high-density polyribosomes (Fig. 2, strain PHLS probed with *PHLS* primers). In contrast, transcripts from the *cpcB·PHLS* construct showed uneven distribution and a gradient with a greater number of low-density than high-density polyribosomes (Fig. 2, strain cpcB·PHLS probed with *PHLS* primers). Transcripts from the *cpcB·PHLS* construct also showed uneven distribution, and a gradient with a greater number of low-density than high-density polyribosomes, when probed with *cpcB* primers (Fig. 2, strain cpcB·PHLS probed with *cpcB* primers). The polyribosomes profile associated with the *cpcB·PHLS*

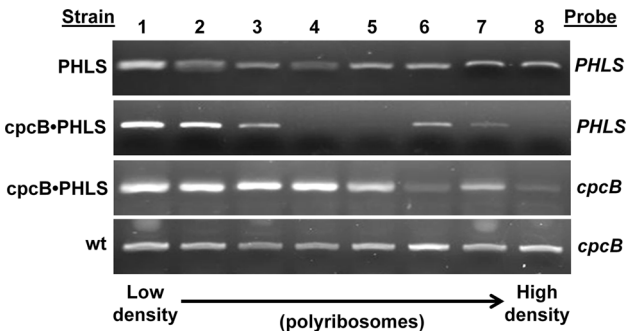

Fig. 2 Analysis of polyribosome density associated with the *PHLS* or *cpcB·PHLS* transcripts, or the endogenous wild-type (wt) *cpc* operon transcripts. *Synechocystis* total cell-cleared lysates were resolved in a 10–40 % sucrose gradient ultracentrifugation. Fractions obtained were numbered from low-to-high sucrose gradient density (1 through 8, respectively), corresponding to low-density and high-density polyribosomes. Semi-quantitative RT-PCR was performed on each gradient fraction derived from the *PHLS, cpcB·PHLS*, or the wild-type (wt) strains with the *PHLS* or the *cpcB* encoding sequences serving as probes (specified on the right side of the figure). This experiment was reproducibly repeated with three independent biological replicates, and representative results are shown

transcripts was therefore reproducible in separate measurements regardless of whether primers specific to *cpcB* or *PHLS* encoding sequences were used to probe the polyribosome assembly. These results suggested a shorter dwell time of ribosomes on the *cpcB·PHLS* transcript compared to the *PHLS* construct.

Figure 2 additionally shows the polyribosomes profile of the *cpc* operon transcript in the wild type, probed with *cpcB* primers. The *cpc* operon transcript is associated evenly with low-density and high-density polyribosomes (Fig. 2, wt). The lower density polyribosomes associated to the *cpcB·PHLS* transcript, compared to the *cpc* operon transcript in the wild type, are probably a consequence of the *cpcB·PHLS* construct configuration. This construct was inserted in the *cpc* genomic locus, while maintaining the subsequent *cpc* operon genes in place (Fig. 1c). The *cpcB·PHLS-cmR* construct may have caused a ribosome drop-off at the end of the *cpcB·PHLS-cmR* encoding sequence, thus reducing the ribosomes density on the respective mRNA. This explanation is consistent with the overexpression of the CpcB·PHLS and CmR proteins, and the substantially lower expression of the subsequent CpcA protein in these transformants (Formighieri and Melis 2015).

Stabilities of the PHLS and CpcB·PHLS recombinant proteins in cyanobacteria

Protein stability and turnover in *Synechocystis* were assessed upon inhibition of *de novo* protein biosynthesis in a time-course analysis. Culture aliquots from wild-type and transformant cyanobacteria were removed at different time points after kanamycin addition to the culture. The cells were immediately disrupted, and pellet and supernatant fractions were separated by centrifugation. Proteins were extracted from the two fractions and examined by SDS-PAGE and Western blot analysis (Fig. 3). Since terpene synthases precipitate upon centrifugation, probably because they adhere to the surface of cellular membranes (Formighieri and Melis 2015), the pellet fractions from wild type and the transformants expressing PHLS or CpcB·PHLS are emphasized in Fig. 3. Qualitatively similar results were obtained with the cyanobacterial supernatant fractions (Fig. 1S, Supplementary material), although the amount of CpcB·PHLS in this fraction was much lower relative to that measured with the pellet fraction.

Lanes 1, 2, 3, and 4 in Fig. 3 correspond to 0, 5, 24, and 96 h of cell incubation in the presence of kanamycin, respectively. While the PHLS protein could not be detected upon Coomassie-staining of protein extracts (Fig. 3a, PHLS), the CpcB·PHLS fusion was particularly abundant in the corresponding transformants as an 82 kD band, and its accumulation was stable in the course of 24 h of protein

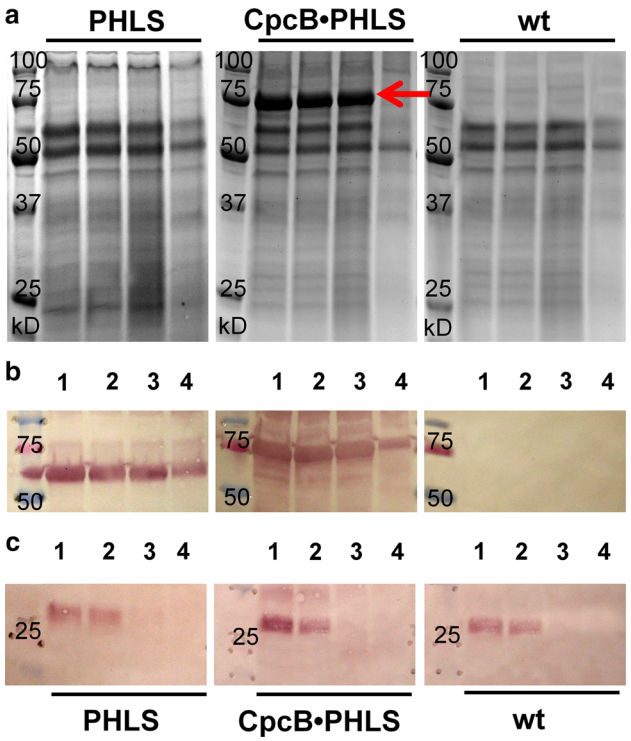

Fig. 3 Time-course analysis of cellular protein levels upon protein synthesis inhibition in the *PHLS* and *CpcB·PHLS* transformants, and in the wild type (wt). Cultures at $OD_{730\ nm}$ of ~0.9 were treated with 50 μg/mL of kanamycin to inhibit protein biosynthesis. Kanamycin was used in this experiment as *Synechocystis* transformants contain the chloramphenicol resistance selection cassette. Cells were harvested prior to kanamycin addition (*lanes 1*), and after 5 h (*lanes 2*), 24 h (*lanes 3*), and 96 h (*lanes 4*) of kanamycin incubation. Pellet fractions upon centrifugation of cell lysates were resolved by SDS-PAGE and Coomassie-stained (**a**), or transferred to nitrocellulose prior to crossreaction with specific antibodies raised against the PHLS (**b**), or the D1/32 kD reaction center protein of PSII (**c**). The CpcB·PHLS fusion protein is pointed by a red arrow. Molecular weight markers are given in kD

synthesis inhibition (Fig. 3a, red arrow). Loss of total protein is seen in the samples from cells incubated for 96 h in the presence of the protein synthesis inhibitor, attributed to culture deterioration in the presence of the antibiotic over such a long period of time (Fig. 3, lanes 4).

Western blot analysis tested for levels of the PHLS protein as a 64 kD band (Fig. 3b, PHLS) or a 75 kD fusion band (Fig. 3b, CpcB·PHLS fusion). Evident from the results is the stability of both the PHLS and CpcB·PHLS proteins, as a function of incubation time (0–24 h) in the presence of kanamycin. A test of the efficiency of protein synthesis inhibition was conducted in Western blot analysis of the above samples with specific polyclonal antibodies recognizing the D1/32 kD protein of PSII (Fig. 3c). The D1 protein is normally subject to frequent turnover in the light, as part of PSII damage and repair cycle (Mattoo and Edelman 1987; Guenther and Melis 1990), and it was chosen as reference for

the protein synthesis inhibition employed in this study. Results showed that the amount of D1 declined in the pellet fraction with similar kinetics in all three samples, to the point where less than 50 % of D1 remained after 5-h incubation in the presence of kanamycin, and 100 % of it was lost after 24-h incubation (Fig. 3c).

The above investigations of gene expression and protein accumulation showed overall similar transcripts abundance for *PHLS* and *cpcB·PHLS*, when these are expressed under the control of the *cpc* promoter. The corresponding recombinant proteins were equally stable against proteolysis. Differences in the expression of the *PHLS* and *cpcB·PHLS* genes were only observed in the polyribosomes profile of the corresponding mRNAs, which likely reflect different rates and efficiencies of protein biosynthesis, ultimately accounting for the substantially different steady-state level of the two recombinant proteins under our growth conditions.

Constructs for carbon-flux amplification in the terpenoid biosynthetic pathway of cyanobacteria

Strains highly expressing the *cpcB·PHLS* transgene satisfy the requirement of abundance in the amount of the PHLS terpene synthase, as a means by which to counter the slow k_{cat} of the enzyme. The *cpcB·PHLS* transformant was then used as recipient for heterologous co-expression of the geranyl-diphosphate synthase (GPPS) and of the enzymes of the MVA pathway. This approach was designed to increase carbon flux in the terpenoid biosynthetic pathway (Bentley et al. 2014) and, therefore, improve substrate availability for the biosynthesis of β-phellandrene. In particular, codon-optimized genes for GPPS and the enzymes of the MVA pathway were divided in two operon constructs, corresponding to the upper and the lower parts of the MVA pathway (Bentley et al. 2014). The operon encoding the upper portion of the MVA pathway (Fig. 4, upper panel), including the HMGS, HMGR, ATOB, and the kanamycin resistance cassette KmR, was inserted via double homologous recombination in the *psbA2* genomic locus, operated under the control of the endogenous *psbA2* promoter and upon replacement of the native *psbA2* gene. The operon encoding the lower MVA pathway (Fig. 4, lower panel), including the GPPS, FNI, MK, PMD, PMK, and a streptomycin resistance cassette SmR, was inserted via double homologous recombination in the *glgA1* genomic locus, upon replacement of the native *glgA1* gene, and operated under the control of the heterologous Ptrc promoter (Formighieri and Melis 2014b). In this case, the GPP synthase from *Picea abies* (Formighieri and Melis 2014a) was cloned upstream of the lower MVA genes in operon configuration.

Transgene genomic DNA insertion and homoplasmy

Attainment of transgenic DNA copy homoplasmy in the above transformants was tested by genomic DNA PCR analysis (Fig. 5). Oligonucleotide primers employed are shown as arrows in Figs. 1 and 4, and corresponding sequences are reported in the Supplementary material, Table 1S. By using primers cpc_us and cpcA_Rv, annealing upstream of the *cpc* operon promoter and within the *cpcA* gene, respectively, the PCR reaction generated the correct 3735 bp products in the cpcB·PHLS and MVA co-transformants, and a 1289 bp product in the wild type (Fig. 5a). The larger product size of the former is due to the *cpcB·PHLS* fusion and cmR cassette insert. Integration of the *cpcB·PHLS* construct in the *cpc* locus was additionally verified with primers cpc_us and PHLS_Rv, annealing upstream of the *cpc* operon and within the *PHLS* sequence, respectively, and resulting in the correct 1927 bp product (Fig. 5b). No PCR product was generated with these primers in the wild type (Fig. 5b, wt).

By using primers psbA2_us and psbA2_ds, annealing upstream and downstream of the *psbA2* locus, respectively, the PCR reaction generated the correct 6321 bp product in the transformants expressing the *upper* MVA pathway in place of the native *psbA2* gene (Fig. 5c). The strain expressing the *cpcB·PHLS* fusion only, referred to as the recipient strain (Fig. 5c, R), and the wild type (Fig. 5c, wt), gave a PCR product of 2725 bp with these primers, corresponding to the native *psbA2* gene. Integration of the *upper* MVA pathway was additionally tested with primers psbA2_us and HMGS_Rv, annealing upstream of the *psbA2* locus and within the heterologous *HMGS* gene, resulting in the correct PCR product of 1251 bp in the MVA transformants (Fig. 5d). No PCR product was generated with these primers in the recipient strain expressing the *cpcB·PHLS* fusion only and in the wild type (Fig. 5d, R, wt).

By using primers glgA1_us and glgA1_ds, annealing upstream and downstream of the *glgA1* locus, respectively, the correct PCR product of 7552 bp was obtained with the transformants expressing the GPPS, the *lower* MVA pathway, and the SmR cassette in place of the native *glgA1* gene (Fig. 5e). Strains with the *cpcB·PHLS* fusion only and the wild type, where no modification was made to the *glgA1* locus, amplified the native 2468 bp product (Fig. 5e, R, wt). Integration of the GPPS and of the *lower* MVA pathway was additionally tested with primers glgA1_us and FNI_Rv, annealing upstream of the *glgA1* locus and within the heterologous *FNI* gene, respectively, and resulting in the correct PCR product of 1842 bp in the MVA transformants (Fig. 5f). No PCR product was obtained with these primers in the recipient strain expressing the *cpcB·PHLS* fusion only and in the wild type (Fig. 5f, R, wt). Overall, the absence of wild-type products

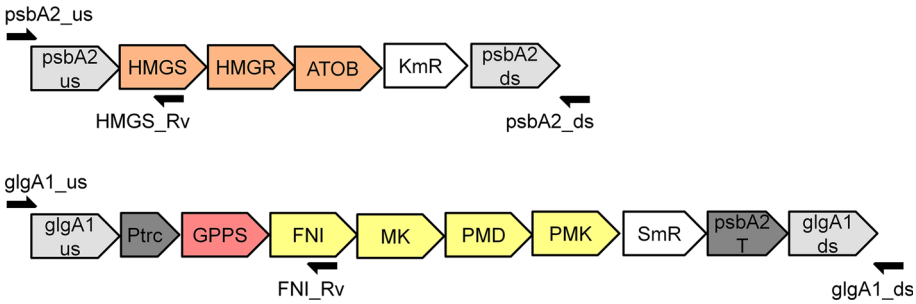

Fig. 4 Schematic of DNA constructs for recombinant expression of the *upper* and *lower* MVA biosynthetic pathway in *Synechocystis*. The *upper* MVA operon was expressed under the *psbA2* promoter upon homologous recombination and replacement of the endogenous *psbA2* gene. The *GPPS* gene, along with the *lower* MVA operon, was expressed under the heterologous Ptrc promoter upon homologous recombination and replacement of the endogenous *glgA1* gene. The 3-hydroxy-3-methylglutaryl-CoA synthase (*HMGS*) and 3-hydroxy-3-methylglutaryl-CoA reductase (*HMGR*) genes were obtained from *Enterococcus faecalis*. The acetyl-CoA acetyl transferase (*ATOB*) gene was from *E. coli*. The geranyl-diphosphate synthase (*GPPS2*) was obtained from *Picea abies*. The isopentenyl-diphosphate isomerase (*FNI*), mevalonic acid kinase (*MK*), di-phospho-mevalonic acid decarboxylase (PMD), and phospho-mevalonic acid kinase (*PMK*) genes were from *Streptococcus pneumoniae R6*. *Arrows mark* oligonucleotide primers used to genetically characterize the transformants

in the PCR reactions of *Synechocystis* M1, M2, and M3 transformants (Fig. 5a, c, e) showed correct genomic integration of the recombinant constructs and attainment of transgenic DNA copy homoplasmy.

Transgenic protein expression in *Synechocystis* transformants

Protein expression in wild-type and *Synechocystis* transformants harboring the CpcB·PHLS fusion, heterologous GPPS, and the MVA pathway enzymes, was assayed by SDS-PAGE and Western blot analysis of total cell extracts, probed with specific polyclonal antibodies (Fig. 6). Results of the Coomassie-stained SDS-PAGE (Fig. 6, top panel) showed that the CpcB·PHLS fusion is the most abundant protein in total cell extracts of *Synechocystis* transformants. Heterologously expressed GPPS and MVA pathway proteins were not clearly distinguishable in the Coomassie-stained SDS-PAGE, but they were present in the *Synechocystis* transformants, as evidenced by their detection in Western blot analysis with specific polyclonal antibodies raised against each of these proteins (Fig. 6).

β-Phellandrene productivity in *Synechocystis* transformants

Overexpression of the CpcB·PHLS fusion protein up to 20 % of total cell protein was a pre-requisite to substantially enhance β-phellandrene product yields over what was measured with transformants harboring limited amounts of the β-phellandrene synthase (Formighieri and Melis 2015). In the present study, rates and yield of β-phellandrene generation were further improved in the *Synechocystis* strains co-expressing the CpcB·PHLS fusion along with the heterologous enzymes of the MVA pathway and the GPP synthase. β-Phellandrene production was measured after 48-h incubation of cultures in the light. The terpene hydrocarbon product was collected as a nonmiscible compound floating on top of the aqueous medium. It was siphoned-off after dilution with a known amount of hexane solvent, which was applied as an over-layer to the surface of the cultures. β-Phellandrene was quantified from the hexane extracts of *Synechocystis* transformant cultures by its specific absorbance in the UV region of the spectrum, showing a primary absorbance band at 232.4 nm (Fig. 7). In contrast, wild-type culture extracts showed no absorbance in the same wavelength region of the spectrum, as wild-type cyanobacteria are not endowed with the synthesis of secondary terpenoids, such as monoterpene hydrocarbons (Fig. 7, wt). Heterologous co-expression of GPPS and the MVA pathway enzymes improved the yield of β-phellandrene production by at least 2-fold over that measured from transformants with the CpcB·PHLS construct only (Fig. 7, CpcB·PHLS + GPPS + MVA vs. CpcB·PHLS). Systematic quantification of β-phellandrene production with independent transformants and multiple replicates showed an average of 10 mg of β-phellandrene per g of dry biomass produced during the 48-h incubation period, corresponding to a ~1 % β-phellandrene:biomass (w:w) carbon-partitioning ratio (Table 1, CpcB·PHLS + GPPS + MVA).

Proper identification of the chemical product in the hexane extract, emanating from the CpcB·PHLS + GPPS + MVA and CpcB·PHLS transformants, was implemented by GC-FID analysis. The results of this analysis are shown in Fig. 8, where a β-phellandrene standard showed a major peak with a retention time of 15.039 min, under our experimental conditions (Fig. 8, *upper panel*). Hexane extracts from the *Synechocystis* transformants also showed a major β-phellandrene peak with a retention time of 15.315 min (Fig. 8, *lower* panel). A smaller amount of β-

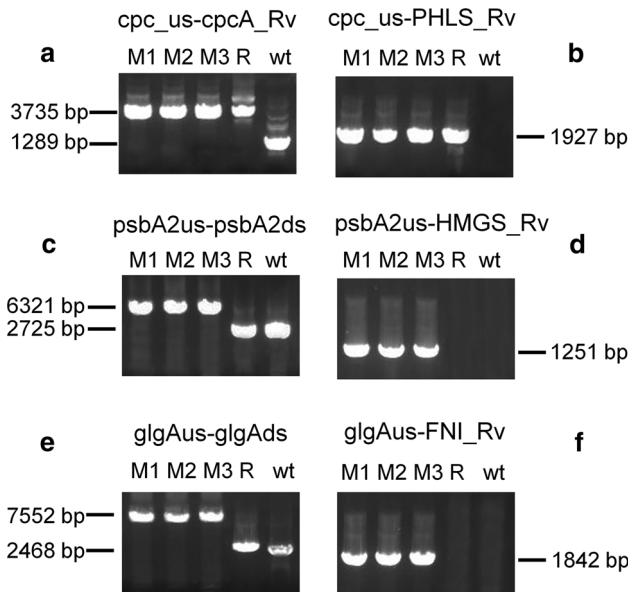

Fig. 5 Genomic DNA PCR analysis with selected forward and reverse primers positioned on the genomic DNA of *Synechocystis* wild-type (wt) and *PHLS* transformants. M1, M2, and M3 refer to the three independent transformant lines co-expressing GPPS and the MVA pathway in addition to the CpcB·PHLS fusion. Strains expressing the CpcB·PHLS only are referred to as the recipient strains (R). **a** PCR reaction using primers cpc_us and cpcA_Rv, amplifying the *cpc* promoter-to-*cpcA* genomic region. **b** PCR reaction using primers cpc_us and PHLS_Rv, amplifying the *cpc* promoter-to-*PHLS* transgene genomic region, and designed to test for integration of *PHLS* in the transformants. **c** PCR reaction using primers psbA2_us and psbA2_ds, amplifying the *psbA2* promoter-to-*psbA2* terminator region. **d** PCR reaction using primers psbA2_us and HMGS_Rv, amplifying the *psbA2* promoter-to-*HMGS* transgene genomic region, and designed to test for integration of the *upper* MVA recombinant construct in the transformants. **e** PCR reactions using primers glgA1_us and glgA1_ds, amplifying the *glgA1* locus. **f** PCR reactions using primers glgA1_us and FNI_Rv, amplifying the *glgA1* upstream-to-*FNI* transgene genomic region, and designed to test for integration of the *lower* MVA recombinant construct in the transformants

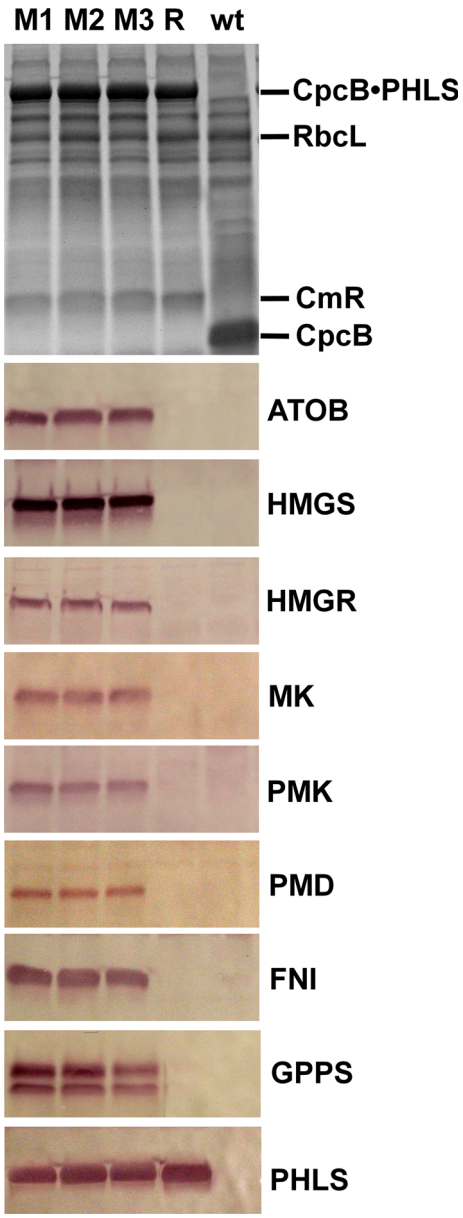

Fig. 6 Protein expression analysis of *Synechocystis* wild type and transformants. Total cell proteins were resolved by SDS-PAGE and Coomassie-stained (*upper panel*), or transferred to nitrocellulose and probed with specific polyclonal antibodies. Individual heterologous proteins are specified on the *right side* of the figure. M1, M2, and M3 refer to the three independent transformant lines co-expressing CpcB·PHLS, GPPS, and the enzymes of the MVA pathway. The strain expressing the CpcB·PHLS only is referred to as the recipient strain (R). Wild-type *Synechocystis* extracts are also shown (wt)

myrcene was detected in the hexane extract of the transformants, apparently the byproduct of the recombinant PHLS enzymatic activity, consistent with previous results (Formighieri and Melis 2014a, 2015).

Discussion

Exploitation of cyanobacteria for heterologous production of terpene hydrocarbons with industrial application requires the ability to generate these products with a relatively high yield. However, terpene synthases are rather slow enzymes, with k_{cat} of 4 s^{-1}, or slower (Demissie et al. 2011; Rajaonarivony et al. 1992; Schilmiller et al. 2009), necessitating high levels of enzyme concentration to enable meaningful rates and yield of product formation (Formighieri and Melis 2015). Moreover, the endogenous terpenoid biosynthetic pathway comprises a limited and highly regulated flux accounting for only 4–5 % of all photosynthetically fixed carbon in cyanobacteria, compared to ~85 % of carbon flux that is directed toward carbohydrate synthesis (Lindberg et al. 2010). As a

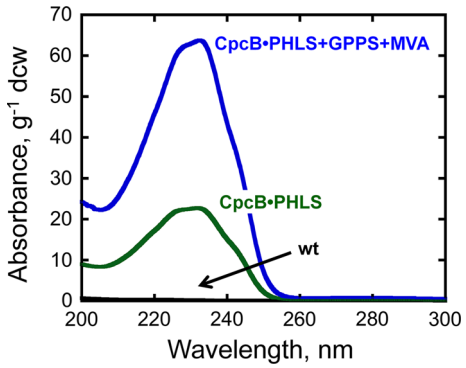

Fig. 7 Detection of β-phellandrene hydrocarbons production by *Synechocystis* transformants. β-Phellandrene from strains expressing the CpcB·PHLS construct are compared to those heterologously co-expressing CpcB·PHLS with GPPS and the MVA pathway (CpcB·PHLS + GPPS + MVA). β-Phellandrene was collected as a nonmiscible compound floating on top of the aqueous phase of *Synechocystis* cultures and siphoned off after applying a hexane solvent over-layer. Absorbance spectra of the hexane extracts are shown, which were normalized on per g of dry cell weight (dcw) of the photosynthesizing biomass. Averages were calculated from three independent biological replicates for each genotype. In contrast to *Synechocystis* transformants, no β-phellandrene was detected in wild-type cultures

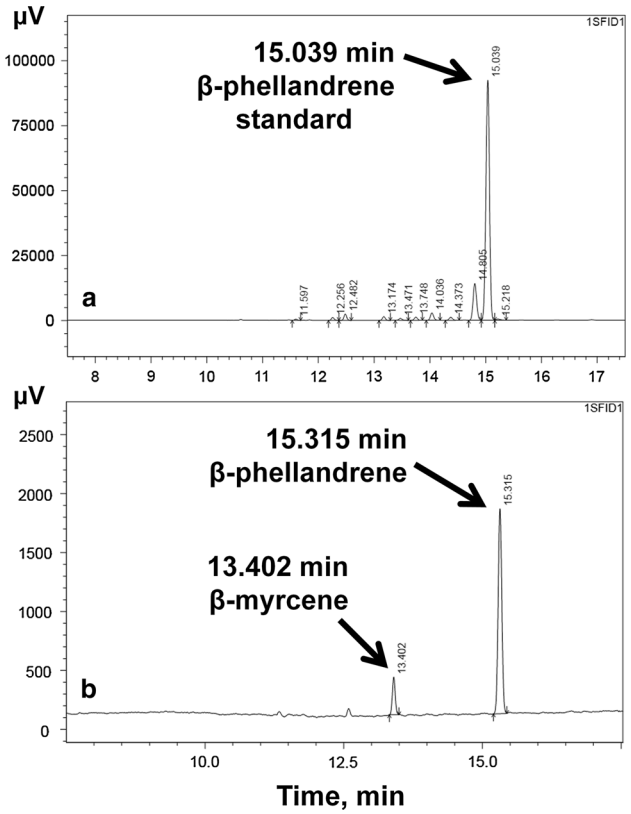

Fig. 8 GC-FID analysis of hexane extracts from *Synechocystis* transformants. **a** GC-FID analysis of a β-phellandrene standard (Chemos GmbH), showing a retention time of 15.039 min under these experimental conditions. **b** GC-FID analysis of hexane extracts from *Synechocystis* transformant cultures heterologously co-expressing CpcB·PHLS with the GPPS and MVA pathway enzymes. β-Phellandrene was the major terpene hydrocarbon product, showing a retention time of 15.315 min under these experimental conditions. Smaller amounts of β-myrcene with a retention time of 13.402 min were also detected as a second product of the PHLS catalysis in the transformants. GC-FID analysis of hexane extracts from wild-type cultures displayed a flat profile, showing no discernible peaks in the 5–20-min retention-time region (not shown)

consequence, metabolic engineering to increase carbon flux through the terpenoid biosynthetic pathway is also needed.

In the present study, we investigated aspects of terpene synthase gene transcription, mRNA accumulation, and protein synthesis and stability, as these affect the accumulation of the recombinant proteins. This is an important issue for the field as transgenes, and especially transgenes of plant origin, are not always expressed to significant levels in cyanobacteria (Formighieri and Melis 2015). Based on our results, the choice of a strong promoter, such as *cpc*, was necessary but not sufficient to enable high levels of terpene synthase expression in cyanobacteria.

Table 1 Photosynthetic carbon partitioning between β-phellandrene and cellular biomass in *Synechocystis*

Genotype	β-Phellandrene yield (mg g^{-1} dcw)		
	Transformant lines tested		
	a	b	c
ΔCpc + PHLS	0.50 ± 0.08	0.43 ± 0.16	0.33 ± 0.06
CpcB·PHLS	5.96 ± 1.22	4.60 ± 1.26	4.47 ± 0.74
CpcB·PHLS + GPPS	6.68 ± 0.84	5.78 ± 1.03	4.90 ± 0.73
CpcB·PHLS + GPPS + MVA	12.44 ± 4.21	10.86 ± 3.54	9.22 ± 1.07

Yields are expressed as mg of β-phellandrene relative to the increment in biomass observed during a 48-h culture incubation period. Three independent transformant lines were assayed for each genotype, with corresponding averages and standard deviations listed. *ΔCpc + PHLS* denotes a transformant in which the *cpc* operon was replaced by the *PHLS* transgenic construct. *CpcB·PHLS* denotes a transformant expressing the *cpcB·PHLS* fusion in the *cpc* genomic locus. *CpcB·PHLS + GPPS* denotes the additional expression of the *GPPS* gene in the background of the *cpcB·PHLS* fusion construct. *CpcB·PHLS + GPPS + MVA* denotes the additional expression of the *GPPS* gene and of the MVA pathway genes in the background of the *cpcB·PHLS* fusion construct. All strains have a ΔCpc phenotype, failing to assemble the phycobilisome

Protein stability was also not an issue in PHLS accumulation, as the latter is a heterologous protein and, therefore, may not be subject to physiological regulations or recognition by the cellular degradation machinery. In contrast, our results point to the importance of efficient translation and protein synthesis in the accumulation of heterologous proteins in cyanobacteria.

The study showed that the *PHLS* transcript was associated with higher density polyribosomes than the *cpcB·PHLS* fusion construct (Fig. 2). Given the shorter *PHLS* transcript, the expectation was that ribosome dwell-time would be correspondingly shorter in this construct (Qin and Fredrick 2013). However, we observed high-density polyribosomes, suggesting slow ribosome migration and pile-up during translation, consistent with the measured lower relative accumulation of the PHLS protein. In contrast, the *cpcB·PHLS* transcript was associated with lower density polyribosomes, compared to either the *PHLS* or the native *cpc* operon transcripts (Fig. 2). This could be attributed to a possible ribosome drop-off at the end of the *cpcB·PHLS* + *cmR* construct, compared with the native *cpc* operon, consistent with the higher accumulation of the CpcB·PHLS and CmR proteins and the lower accumulation of the downstream CpcA protein (Formighieri and Melis 2015). In addition, given the high level of CpcB·PHLS protein accumulation compared to PHLS, it is also suggested that *cpcB*, as an endogenous sequence that is highly expressed, helps enhance ribosome migration and translation through both the leading *cpcB* and trailing *PHLS* in the *cpcB·PHLS* fusion construct.

In contrast to the positive results obtained upon fusion of the *PHLS* sequence to the entire *cpcB* gene, fusion of PHLS to the leading 10 amino acids of the CpcB sequence did not bring about enhanced expression of the recombinant protein (results not shown). Codons immediately downstream of the translation initiation were shown to affect accumulation of heterologous proteins by defining the efficiency of translation initiation (Kuroda and Maliga 2001a, b; Formighieri and Melis 2014b). However, translation initiation was not the main determinant in recombinant protein expression in this study, and the benefit of the upstream *cpcB* moiety required the entire *cpcB* encoding sequence.

Carbon flux through the terpenoid biosynthetic pathway and toward the synthesis of desired terpene hydrocarbons is another important determinant of yield. The PHLS enzyme converts GPP into the cyclic monoterpene β-phellandrene. However, heterologous co-expression of the GPP synthase with the CpcB·PHLS fusion protein did not significantly improve β-phellandrene yields, compared to the strain expressing the CpcB·PHLS only (Table 1, CpcB·PHLS + GPPS). In contrast, the combination of CpcB·PHLS, GPPS, and the complete MVA pathway, when expressed in the same cyanobacterial transformant, resulted in at least 2-fold increase in β-phellandrene product yield, compared to the CpcB·PHLS strain, reaching about 10 mg of β-phellandrene accumulated per g of dcw produced during the same incubation period, i.e., ~1 % β-phellandrene:biomass carbon-partitioning ratio (Fig. 7; Table 1, CpcB·PHLS + GPPS + MVA). An advantage of this approach lies in enhanced carbon-flux through the terpenoid biosynthetic pathway, by acting on upstream metabolic reactions, thereby adding to the pools of IPP and DMAPP precursors and, consequently, to GPP availability. This ultimately translated in improved monoterpene hydrocarbons production. It is worth noting that all strains examined in the present study displayed a ΔCpc phenotype, failing to assemble the phycobilisome, as already reported for the CpcB·PHLS transformant (Formighieri and Melis 2015).

An assessment of the influence of different molecular genetic and biochemical variables in β-phellandrene product generation, relative to cyanobacteria biomass accumulation, is given in the results of Fig. 9. By using strong promoters and suitable translation initiation regions in association with the β-phellandrene synthase transgene, yields in the range of 0.01–0.25 mg of β-PHL per g dcw were achieved (Formighieri and Melis 2014b). Overexpression of the recombinant β-phellandrene synthase to levels exceeding 5 % of the total cellular protein, when

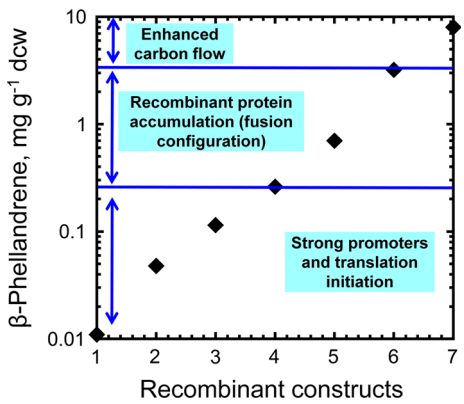

Fig. 9 Graphic depiction of progress in the yield of β-phellandrene production. Strong promoters, application of translation initiation regions, protein fusion configurations for transgenic protein accumulation, and enhanced cellular substrate flux toward IPP and DMAPP, all contributed to increased β-phellandrene production and enhanced β-PHL:biomass carbon-partitioning ratio. In this graph, product formation is expressed in a logarithmic scale as mg of β-phellandrene per g of dry weight of cellular biomass accumulated over a 48-h culture incubation period. Constructs 1, 2, 3, and 4 refer to the use of different strong promoters and translation initiation regions, as described (Formighieri and Melis 2014b). Constructs 5 and 6 refer to transgenic protein fusion configurations that allowed for substantial PHLS protein accumulation (Formighieri and Melis 2015). Construct 7 shows the effect of co-expression of the CpcB·PHLS fusion construct along with heterologous GPPS and MVA pathway in *Synechocystis* (this study)

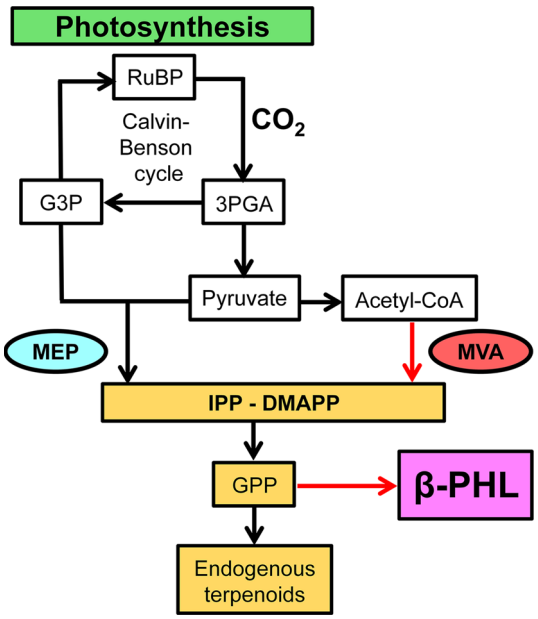

Fig. 10 Schematic of metabolic pathways in *Synechocystis* transformants, as employed in this study. Photosynthetically assimilated CO_2 yields 3-phosphoglyceric acid (3PGA), which is converted into glyceraldehyde 3-phosphate (G3P) or pyruvate. Pyruvate and G3P are the primary reactants of the *Synechocystis* endogenous methylerythritol (MEP) biosynthetic pathway leading to the synthesis of the 5-carbon intermediates isopentenyl-diphosphate (IPP) and dimethylallyl diphosphate (DMAPP). Pyruvate decarboxylation leads to acetyl-CoA formation, which is the primary reactant of the heterologous mevalonic acid (MVA) pathway, also leading to the synthesis of IPP and DMAPP. Covalent linkage of IPP and DMAPP yields geranyl-diphosphate, a 10-carbon terpenoid intermediate metabolite, *en route* toward the generation of longer chain endogenous terpenoids (carotenoids, phytol, and quinone prenyl tails, among others). Heterologous expression of the *PHLS* gene drains a portion of the GPP pool toward the synthesis of β-phellandrene that spontaneously diffuses out of the cyanobacterial cell. The flow of endogenous carbon substrate toward the terpenoid biosynthetic pathway was enhanced upon heterologous expression of the MVA pathway in *Synechocystis*, increasing the pool size of IPP and DMAPP substrate. Endogenous and heterologous reactions are delineated in *black* and *red*, respectively

implemented in addition to strong promoters, enhanced yields from 0.25 mg of β-PHL per g dcw upward to about 3 mg of β-PHL per g dcw (Formighieri and Melis 2015). Further improvements in yield, up to about 10 mg of β-PHL per g dcw, were achieved upon heterologous carbon flow through the MVA pathway (Fig. 9). These results suggest a major limitation in monoterpene hydrocarbons' production due to the slow k_{cat} of the monoterpene synthase enzyme and relative enzyme concentration, and an additional limitation due to substrate availability. Monoterpene synthases were reported to have relatively low K_M of 2–10 μM (Demissie et al. 2011; Rajaonarivony et al. 1992, Schilmiller et al. 2009). Nonetheless, the higher β-PHL yield that was observed upon increasing substrate availability, through expression of the entire MVA pathway in *Synechocystis*, suggests that the endogenous steady-state GPP concentration in cyanobacteria is lower than what is required for the saturation of the β-phellandrene synthase, thus limiting β-PHL production.

In summary, this study has shown the ability to enhance yields of β-phellandrene synthesis upon overexpression of the β-phellandrene synthase, and upon the concomitant improvement in endogenous substrate flux to IPP/DMAPP via the heterologous expression of the MVA pathway in the cells (Fig. 10). It is of interest that even a low level of expression of the MVA pathway in *Synechocystis*, to the point where protein bands were not visible upon Coomassie-staining of total cell extracts (Fig. 6), did suffice to divert considerable amounts of photosynthetically fixed carbon toward the terpenoid biosynthetic pathway. Future efforts, aimed at optimizing the expression of the MVA pathway in cyanobacteria, may further increase carbon partitioning and product yields. Approaches employed in this study would be useful in the effort to achieve meaningful rates and yield of product formation, leading to a commercially successful application of cyanobacteria as platforms for the generation of commodity products, such as terpene hydrocarbons.

References

Alonso-Gutierrez J, Chan R, Batth TS, Adams PD, Keasling JD, Petzold CJ, Lee TS (2013) Metabolic engineering of *Escherichia coli* for limonene and perillyl alcohol production. Metab Eng 19:33–41

Bar-Even A, Noor E, Savir Y, Liebermeister W, Davidi D, Tawfik DS, Milo R (2011) The moderately efficient enzyme: evolutionary and physicochemical trends shaping enzyme parameters. Biochemistry 50:4402–4410

Bentley FK, Melis A (2012) Diffusion-based process for carbon dioxide uptake and isoprene emission in gaseous/aqueous two-phase photobioreactors by photosynthetic microorganisms. Biotechnol Bioeng 109:100–109

Bentley FK, García-Cerdán JG, Chen HC, Melis A (2013) Paradigm of monoterpene (β-phellandrene) hydrocarbons production via photosynthesis in cyanobacteria. BioEnergy Res 6:917–929

Bentley FK, Zurbriggen A, Melis A (2014) Heterologous expression of the mevalonic acid pathway in cyanobacteria enhances endogenous carbon partitioning to isoprene. Mol Plant 7:71–86

Davies FK, Work VH, Beliaev AS, Posewitz MC (2014) Engineering limonene and bisabolene production in wild type and a glycogen-deficient mutant of *Synechococcus* sp. PCC 7002. Front Bioeng Biotechnol 2:21

Demissie ZA, Sarker LS, Mahmoud SS (2011) Cloning and functional characterization of β-phellandrene synthase from *Lavandula angustifolia*. Planta 233:685–696

Duetz WA, Bouwmeester H, van Beilen JB, Witholt B (2003) Biotransformation of limonene by bacteria, fungi, yeasts, and plants. Appl Microbiol Biotechnol 61:269–277

Eaton-Rye JJ (2011) Construction of gene interruptions and gene deletions in the cyanobacterium *Synechocystis* sp. strain PCC 6803. Methods Mol Biol 684:295–312

Farmer WR, Liao JC (2001) Precursor balancing for metabolic engineering of lycopene production in *Escherichia coli*. Biotechnol Prog 17:57–61

Fischer MJC, Meyer S, Claudel P, Bergdoll M, Karst F (2011) Metabolic engineering of monoterpene synthesis in yeast. Biotechnol Bioeng 108:1883–1892

Formighieri C, Melis A (2014a) Carbon partitioning to the terpenoid biosynthetic pathway enables heterologous β-phellandrene production in *Escherichia coli* cultures. Arch Microbiol 196:853–861

Formighieri C, Melis A (2014b) Regulation of β-phellandrene synthase gene expression, recombinant protein accumulation, and monoterpene hydrocarbons production in *Synechocystis* transformants. Planta 240:309–324

Formighieri C, Melis A (2015) A phycocyanin·phellandrene synthase fusion enhances recombinant protein expression and β-phellandrene (monoterpene) hydrocarbons production in Synechocystis (cyanobacteria). Metab Eng 32:116–124

Guenther JE, Melis A (1990) The physiological significance of photosystem II heterogeneity in chloroplasts. Photosynth Res 23:105–109

Harvey B, Benjamin G, Wright M, Quintana R (2010) High-density renewable fuels based on the selective dimerization of pinenes. Energy Fuels 24:267–273

Kim SW, Keasling JD (2001) Metabolic engineering of the nonmevalonate isopentenyl diphosphate synthesis pathway in *Escherichia coli* enhances lycopene production. Biotechnol Bioeng 72:408–415

Kirst H, Formighieri C, Melis A (2014) Maximizing photosynthetic efficiency and culture productivity in cyanobacteria upon minimizing the phycobilisome light-harvesting antenna size. Biochim Biophys Acta 1837:1653–1664

Kuroda H, Maliga P (2001a) Complementarity of the 16S rRNA penultimate stem with sequences downstream of the AUG destabilizes the plastid mRNAs. Nucleic Acids Res 29:970–975

Kuroda H, Maliga P (2001b) Sequences downstream of the translation initiation codon are important determinants of translation efficiency in chloroplasts. Plant Physiol 125:430–436

Lichtenthaler HK (2000) Sterols and isoprenoids. Biochem Soc Trans 28:785–789

Lindberg P, Park S, Melis A (2010) Engineering a platform for photosynthetic isoprene production in cyanobacteria, using *Synechocystis* as the model organism. Metab Eng 12:70–79

Livak KJ, Schmittgen TD (2001) Analysis of relative gene expression data using real-time quantitative PCR and the $2^{-\Delta\Delta CT}$ method. Methods 25:402–408

Martin VJJ, Pitera DJ, Withers ST, Newman JD, Keasling JD (2003) Engineering a mevalonate pathway in *Escherichia coli* for production of terpenoids. Nat Biotechnol 21:796–802

Matthews PD, Wurtzel ET (2000) Metabolic engineering of carotenoid accumulation in *Escherichia coli* by modulation of the isoprenoid precursor pool with expression of deoxyxylulose phosphate synthase. Appl Microbiol Biotechnol 53:396–400

Mattoo AK, Edelman M (1987) Posttranslational palmitoylation of the chloroplast 32-kD herbicide-binding protein. Proc Natl Acad Sci USA 84:1497–1501

Melis A (2013) Carbon partitioning in photosynthesis. Curr Opin Chem Biol 17:453–456

Qin D, Fredrick K (2013) Analysis of polysomes from bacteria. Methods Enzymol 530:159–172

Rajaonarivony JI, Gershenzon J, Croteau R (1992) Characterization and mechanism of (4S)-limonene synthase, a monoterpene cyclase from the glandular trichomes of peppermint (Mentha × piperita). Arch Biochem Biophys 296:49–57

Sarria S, Wong B, Martin HG, Keasling JD, Peralta-Yahya P (2014) Microbial synthesis of pinene. ACS Synth Biol 3:466–475

Schilmiller AL, Schauvinhold I, Larson M, Xu R, Charbonneau AL, Schmidt A, Wilkerson C, Last RL, Pichersky E (2009) Monoterpenes in the glandular trichomes of tomato are synthesized from a neryl diphosphate precursor rather than geranyl diphosphate. Proc Natl Acad Sci USA 106:10865–10870

Stephens E, Ross IL, Hankamer B (2013) Expanding the microalgal industry—continuing controversy or compelling case? Curr Opin Chem Biol 17:444–452

Tracy N, Chen D, Crunkleton DW, Price GL (2009) Hydrogenated monoterpenes as diesel fuel additives. Fuel 88:2238–2240

Van Wagoner RM, Drummond AK, Wright JLC (2007) Biogenetic diversity of cyanobacterial metabolites. Adv Appl Microbiol 61:89–217

Williams JGK (1988) Construction of specific mutations in photosystem II photosynthetic reaction center by genetic engineering methods in *Synechocystis* 6803. Methods Enzymol 167:766–778

Zurbriggen A, Kirst H, Melis A (2012) Isoprene production via the mevalonic acid pathway in *Escherichia coli* (bacteria). BioEnergy Res 5:814–828